

УДК 556.12 : 551.577.35 : 517.444

## SOME ASPECTS OF THE NONLINEAR INTERACTION BETWEEN GLOBAL TELECONNECTION PATTERNS

A.V. Glushkov, N.S. Loboda, V.N. Khokhlov, A.A. Svinarenko, N.G. Serbov, Yu. Bunyakova

*Одесский государственный экологический университет, г. Одесса-9, п/я 24а*

*E-mail: [glushkov@paco.net](mailto:glushkov@paco.net)*

**Abstract.** The chaotic behavior in the global climate system of the Earth and the nonlinear interaction between some teleconnection patterns during different epochs of the twenty century are studied. To study the influence of low frequency variations, the wavelet decomposition is applied. We use the cross-redundancy and Granger causality for detailed components of the wavelet decomposition.

**Key words:** teleconnection patterns wavelet expansion, cross-redundancy and Granger causality.

**Некоторые аспекты нелинейного взаимодействия между глобальными телеконнекционными паттернами.** А.В. Глушков, Н.С. Лобода, В.Н. Хохлов, А.А. Свиноаренко, Н.Г. Сербов, Ю.Г. Буныкова  
**Реферат.** Анализируется хаотическое поведение в глобальной климатической системе Земли и нелинейное взаимодействие между телеконнекционными паттернами на протяжении разных эпох 20-го столетия. Для определения влияния низкочастотных вариаций применен метод вейвлет-разложений. Использована взаимная информация и причинность Грангера для анализа детализованных компонент вейвлет-разложений.

**Деякі аспекти нелінійної взаємодії між глобальними телеконекційними паттернами.** О.В. Глушков, Н.С. Лобода, В.М. Хохлов, А.А. Свиноаренко, М.Г. Сербов, Ю.Г. Буныкова  
**Реферат.** Анализується хаотична поведінка у глобальній кліматичній системі Землі й нелінійна взаємодія між телеконекційними паттернами протягом різних епох 20-го сторіччя. Для визначення впливу низькочастотних варіацій застосовано метод вейвлет-розкладань. Використано взаємну інформацію та причинність Грангера для деталізованих компонентів вейвлет-розкладань.

### 1. Introduction

Studying the physical processes of nonlinear interaction between teleconnection patterns is of a great importance in the modern physics of atmosphere and Earth.. Evidence of chaotic behavior for the relationship between the Arctic Oscillation (AO), Southern Oscillation (SO), and Antarctic Oscillation is earlier discovered. Detailed analysis of this phenomenon is carried out in ref. [1] by using the cross-redundancy and Granger causality and wavelet decomposition. Here we consider some aspects of numerical modelling interaction between teleconnection pattern and use the cross-redundancy and Granger causality for detailed components of the wavelet decomposition, basing on the methods and some results of ref. [1].

The temporal variations of the global temperature (and some other meteorological values, e.g. precipitation) during last 150 years show the vibrations and intermittency of the climate and to some extent the variations of climate over longer periods. This pattern gives the impression of being chaotic and bring to mind the behaviour of the dynamic systems which (in the modern theory of chaos) evolve on complex-structured limit sets present in their phase spaces and have come to be known as "strange attractors". This concept was introduced by Lorenz [5]. In light of the above, the theory of climate variation ought to be the statistical dynamics of the climate system.

The main source of energy for the processes in the climate system of the Earth is incident solar flux. Its intensity at Earth's mean distance from the Sun, according to both terrestrial and extraterrestrial measurements, is equal to  $1360 \pm 20 \text{ W m}^{-2}$ . However, the solar forcing of climate variations on decadal and centennial time scales is too small. Oh *et al.* (2003) showed that the solar irradiance variations due to the well-known 11-year Schwabe (sunspot) and the 80–90-year Gleissberg cycles amount to  $1.5 \text{ W m}^{-2}$  and  $2.25 \text{ W m}^{-2}$ , respectively. Thus, it is impossible to apply the solar forcing as the modulator of climate changes on the aforementioned time scales.

Modern numerical models utilize mainly two approaches allowing physical interpretation for the observed climate variations: the greenhouse forcing of the climate system (see, e.g. Monahan *et al.*, 2000; Voss and Mikolajewicz, 2001) and the response of the climatic system on tropical Pacific sea surface temperature (SST) anomalies (see, e.g. Hannachi, 2001; Hurrell *et al.*, 2004). In the last case, per se, the response of the global coupled atmosphere–ocean system to the El Niño–Southern Oscillation (ENSO) events is modelled. The ENSO itself is the dynamical system of the coherently varying atmosphere and ocean, as well as is the one of most prominent global teleconnection patterns. The ability to represent the atmosphere–ocean (and, in the some cases, the atmosphere–land) interaction is also possessed other main teleconnection patterns such as the North Atlantic Oscillation (NAO) and the Pacific North American pattern (PNA), as well as the so-called annular modes – the Arctic Oscillation (AO) and the Antarctic Oscillation (AAO).

One of conceptual approaches used in the chaos theory consists in the defining of correlation dimension for the time series: the low dimension determines the minimal number for the degree of freedom and, consequently, validates the applicability for the method of nonlinear prediction. Such a method is successfully used in the hydrology for the modelling of annual runoff (see, e.g. Sivakumar, 2001). However, Kawamura *et al.* (1998) showed that the low correlation dimensions are unfortunately absent in the Southern Oscillation (SO) Index time series. The plausible reason is that the length of such time series is still too short. But, the Southern Oscillation Index (SOI) time series is characterized by a fractal power law (Ausloos and Ivanova, 2001). One of the disadvantages of chaos analysis is that the assumption underlying it (deterministic time series without observational noise) are not realistic for the oscillation index data. Thus, we analyze the monthly time series of some from the aforementioned oscillations (SO, AO, and AAO) by means of mutual information (Paluš, 1995) which do not requires those assumptions and have already been applied successfully to time series from very different origins, such as meteorology and physiology (Paluš, 1996; Diks and Mudelsee, 2000).

## 2. Main global teleconnection patterns: some preliminaries

The aim of this section in no circumstances is to describe whole variety for interaction mechanisms and feedbacks (for this, we recommend following reviews: Marshall *et al.*, 2001; Wanner *et al.*, 2001; Turner, 2004) acting between the teleconnection patterns we have selected for the analysis. Rather, the purpose is to show that: a) the indices of the AO, ENSO, and AAO reflect, to some extent, the atmosphere–surface interaction, and b) our choice of the mentioned oscillation is valid for the subsequent analysis.

### 2.1 (a) Arctic Oscillation

The term "Arctic Oscillation" has been introduced (Thompson and Wallace, 1998) to describe the leading structure of SLP variability over the Northern Hemisphere that has the leading mode of circulation variability with deep, barotropic, zonally symmetric structure with a primary centre of action over the Arctic and opposing anomalies in midlatitudes. While the AO is defined as a monthly-mean, extratropical, tropospheric pattern of variability, its influence extends well beyond these categories. It has connections to extreme weather events and long-term climate trends, a distinctive signature in the

tropics, and important connections to the stratosphere. The Arctic Oscillation Index (AOI) can be calculated from sea-level pressure (SLP) anomalies north of 20°N. The high index of the AO (warm phase) is defined as periods of below normal Arctic SLP, enhanced surface westerlies over the North Atlantic, and warmer and wetter than normal conditions in northern Europe. The low index of the AO (cool phase) the weather conditions are opposite.

The Arctic Oscillation is frequently compared to the NAO and PNA. Ambaum *et al.* (2001) compared the definition and interpretation of the AO and NAO. They showed that the NAO reflects the correlations between the surface pressure variability at its centres of action, whereas this is not the case for the AO. The NAO pattern can be identified in a physically consistent way in principal component analysis applied to various fields in the Euro–Atlantic region. A similar identification is found in the Pacific region for the PNA pattern, but no such identification is found here for the AO. Their results suggest that the NAO paradigm may be more physically relevant and robust for Northern Hemisphere variability than is the AO paradigm. However, this does not disqualify many of the physical mechanisms associated with annular modes for explaining the existence of the NAO. Deser (2000) showed that the teleconnectivity between the Arctic and midlatitudes is strongest over the Atlantic sector, and that the temporal coherence between the Atlantic and Pacific midlatitudes is weak, both on intraseasonal and interannual time scales, during the past 50 years. Hence, the "annular" character of the AO is more a reflection of the dominance of its Arctic centre of action than any coordinated behaviour of the Atlantic and Pacific centres of action in the SLP field. Also, the AO time series is nearly indistinguishable from the leading structure of variability in the Atlantic sector (e.g., the NAO): their temporal correlation is 0.95 for monthly SLP anomalies during November–April 1947–97. By using a simple dynamical model for the basic spatial and temporal structure of the largescale modes of intraseasonal variability and associated variations in the zonal index, Vallis *et al.* (2004) showed that the NAO and AO produced by the same mechanism, and are manifestations of the same phenomenon. In the present study we investigate the AO as the main teleconnection pattern in the Northern extratropical latitudes. The NAO is very different in character to the SO, and its predictability – at least on seasonal-to-interannual timescales – is almost certainly much lower. The low latitude response is forced by the low latitude SST anomalies, but the high latitude response is influenced by the extratropical SST anomalies as well as those in the tropics. Furthermore, Sutton *et al.* (2001) found the evidence of nonlinear interaction between the influence of the tropical and extratropical SST anomalies. One can be also noted that the aforementioned SST anomalies tripole exerts the influence on the generation of the 7.7-year variability of the NAO. Similar periodicity was found in ref. [3] for the influence of the NAO and SO on the eddy kinetic energy content in the atmosphere of the Northern tropics and midlatitudes.

## 2.2 (b) El Niño–Southern Oscillation

The El Niño–Southern oscillation is the largest climatic cycle on decadal and sub-decadal time scales and it has a profound effect on not only the weather and oceanic conditions across the tropical Pacific, where the ENSO has its origins, but also in regions far removed from the Pacific basin. ENSO has a very direct influence on weather conditions in some latitude areas, and its effects, for example, have been linked to the anomalies of global precipitation (Dai and Wigley, 2000). The evolution of the ENSO cycle can be measured by a number of different indices. In the present paper, we use the Southern Oscillation index, which is the normalized difference in surface pressure between Tahiti and Darwin, Australia.

As well as for the AO/NAO case, the atmosphere–ocean interaction realizes in the ENSO. For example, by using the wavelet transform, Lucero and Rodríguez (2000) studied the decadal and interdecadal fluctuations in the equatorial Pacific SST and in the SOI. They particularly showed that there is a large correlation between positive (negative) extreme of SOI fluctuations and associated negative (positive) extreme of SST anomaly fluctuations at decadal, bidecadal, and interdecadal timescales. The controlling process on the variability of the decadal components of winter SOI and winter SST anomaly in 1896–1985 is a joint amplitude modulation. This amplitude modulation attains

maximum amplitude in 1913–1917. Thereafter, amplitude decreases until about 1959. In early-1960s, the growing branch of this amplitude modulation for the decadal fluctuations starts. The ENSO have undergone considerable interdecadal changes over the last 125 years. By using the wavelet decomposition, Torrence and Webster (1999) showed that wavelet power spectra and variance time series show interdecadal changes in 2–7-yr variance, and indicate intervals of high variance (1875–1920 and 1960–90) and an interval of low variance (1920–60). Also, the 2–7-yr variance time series contain a 12–20-yr oscillation, consisting of a 12–20-yr modulation of ENSO amplitude. Corresponding to El Niño events, the global atmospheric circulation is modified through the changes of Walker–Hadley circulation (Klein *et al.*, 1999). The SST of remote oceans thus affected. Such effects were detected both for the Atlantic (Wang, 2004) and for the Southern ocean (Li, 2000).

### 2.3 (c) Antarctic Oscillation

Although as early as in the first quarter of this century Sir Gilbert Walker had stated that: "Just as in the North Atlantic there is a pressure opposition between the Azores and Iceland, ..., there is an opposition between the high pressure belt across Chile and the Argentine on the one hand, and the low pressure area of Weddell Sea and the Bellingshausen Sea on the other.", the scarcity of data in the Southern Hemisphere hindered the search for new oscillation(s). During the last two decades, more comprehensive data over the Southern Hemisphere became available, a fourth atmospheric oscillation in the middle and high southern latitudes was found, and named as the Antarctic Oscillation. This term refers to a large scale alternation of atmospheric mass between the mid-latitude and high latitudes.

The AAO emerges as the leading empirical orthogonal function of mean SLP over the Southern Hemisphere with associated regression patterns of temperature, zonal wind, and geopotential height from the surface to the stratosphere. The AAO is, per se, the counterpart of the AO, and the Antarctic Oscillation Index (AAOI) can be calculated from sea-level pressure anomalies south of 20°S.

### 2.4 (d) Forced climate change and teleconnection patterns

The climate change comprises a reversal of the sea surface temperature anomaly pattern in the North Pacific Ocean, a lowering of the atmospheric geopotential height in the North Pacific, altered frequency and intensity of cyclones/anticyclones and severe storms in the mid- and high latitudes, along with an "abrupt" increase of the Northern Hemisphere average surface air temperature. It is naturally that these changes affect the teleconnection pattern. Hu *et al.* (2004) showed that in 1979–2000 the significant increases of the NH summer and winter season kinetic energy, both mean and eddy, have observed in comparison with 1948–78. The increase has resulted from increased conversion rates from the mean to the eddy available potential energy and then from the eddy available potential energy to the eddy and mean kinetic energy. Keeping in mind that the eddy kinetic energy is well correlated with the NAO and ENSO at the long time scale (Khokhlov *et al.*, 2004), one can be concluded that the observed warming affects significant changes in the teleconnection patterns.

Moreover, some simulations with numerical models indicate that the response on the greenhouse forcing is found both for the ENSO and for the annular modes (AO and AAO). For example, Cai and Whetton (2000) reported results from experiments using the CSIRO Mark 2 CGCM which show a warming pattern that is initially La Niña-like, but after the 1960s El Niño-like. Their results show that a linkage between tropical and extratropical ocean circulation can cause an initial warming pattern to change. Also, climate change simulations for the period 1900–2100, with forcing due to greenhouse gases and aerosols, exhibit positive trends in both the AO and the AAO (Fyfe *et al.*, 1999). Their results do not suggest that a simulated trend in the AO/AAO necessarily depends on stratospheric involvement nor that forced climate change will be expressed as a change in the occurrence of one phase of the AO/AAO over another. This pattern of climate change projects exclusively on the AAO pattern in the Southern Hemisphere but not in the Northern Hemisphere. Thus, there is ample evidence that most of the atmospheric circulation variability in the form of the North

Atlantic Oscillation (NAO) arises from the internal, nonlinear dynamics of the extratropical atmosphere (see, e.g. Thompson *et al.*, 2003). From our point of view, such nonlinear dynamics is the characteristic features of whole global atmosphere.

### 3. Data and methodology

#### 3.1 (a) Data

We use unsmoothed datasets for the indices AO, SO, and AAO, as well as for the global temperature anomaly (T) from the base period 1961–90. All data were obtained via Internet ([http://www.jisao.washington.edu/data\\_sets/aots/ao18992002](http://www.jisao.washington.edu/data_sets/aots/ao18992002), <http://www.cru.uea.ac.uk/ftpdaa/soi.dat>, <http://www.jisao.washington.edu/data/aaoslp/aaoslp19482002>, <http://www.cru.uea.ac.uk/ftpdata/tavegl2v.dat>, respectively). From the original datasets, we extract time series from 1910 till 2001 (except for the AAOI that starts from 1948). For further analysis, we divide time series into three epochs: 1910–47, 1948–77, and 1978–2001 (hereafter W1, C, and W2, respectively). First and third epochs are characterized by the global warming while during second epoch the reverse process is observed.

#### 3.2 (b) Mutual information and cross-redundancy

Consider two discrete variables  $X$  and  $Y$  with joint probability density functions (PDF)  $f_{X,Y}(x,y)$ , and marginal PDF  $f_X(x)$  and  $f_Y(y)$  respectively. The mutual information  $I(X, Y)$  quantifies average amount of common information contained in the variables  $X$  and  $Y$ :

$$I(X, Y) = \iint f_{X,Y}(x, y) \log \frac{f_{X,Y}(x, y)}{f_X(x)f_Y(y)} dx dy \quad (1)$$

When the discrete variables  $X$  and  $Y$  from continuous variables on a continuous probability space, then the mutual information depends on a partition chosen to discrete the space. The mutual information can be considered as a nonlinear analogue of the correlation between  $X$  and  $Y$ . The mutual information is symmetric, nonnegative and equal to zero if and only if  $X$  and  $Y$  are independent.

The generalization of mutual information, by expressing it in terms of generalized correlation integrals  $C_q(\varepsilon)$  gives:

$$I_q(X, Y; \varepsilon) = \log C_q(X, Y; \varepsilon) - \log C_q(X; \varepsilon) - \log C_q(Y; \varepsilon). \quad (2)$$

This form enables convenient estimation by means of plug-in estimates of  $C_q$ . The choice  $q = 2$ , value which will be used throughout this paper, is particularly convenient since the estimation of the correlation integral for this case is straightforward. To estimate the correlation integrals, we use the algorithm proposed by Grassberger and Procaccia (1983), which uses the reconstruction of the phase-space. For the scale parameter we chose  $\varepsilon = 0.5$ . Furthermore, to examine the relation between two variables in more detail, we determine the mutual information of time series as a function of the delay (Prichard and Theiler (1995)).

#### 3.3 (c) Granger causality

By using the cross-redundancy, we only examine the dependence between two variables, but not obtain a behaviour of coupling. For example, if there is the nonlinear dependency between two variables, this might be because the first variable is driving the second, or the second is driving the first, or both (feedback). Such a causal relationship can be examined by testing for Granger causality (Granger, 1969). This is well-known concept used in econometrics is based on predictability. According to Granger (1969), the following sentence can be stated.  $Y$  is a Granger cause of  $X$  if past values of  $Y$  can improve predictions of future values of  $X$ , conditionally on past values  $X$  and  $Y$ , are distributed

differently than future values of  $X$  only. In this case  $X$  conditionally (on past values of  $X$ ) dependent on  $Y$ . This definition of causality is only operational and leaves open the possibility that causality is found between  $X$  and  $Y$  when they are in fact uncoupled. This can be the case if both  $X$  and  $Y$  are driven by a third variable (Diks and Mudelsee, 2000).

The above definitions have assumed that only stationary series are involved. In the nonstationary case the existence of causality may alter over time. The definitions can clearly be generalized to be operative for a specified time. One could then talk of causality existing at this moment of time. The one completely unreal aspect of the above definitions is the use of series representing all available information. Let us to illustrate the above definition using model with two variables. Let  $X_t, Y_t$  be two stationary time series with zero means. The simple causal model is

$$\left. \begin{aligned} X_t &= \sum_{j=1}^m a_j X_{t-j} + \sum_{j=1}^m b_j Y_{t-j} + v_t, \\ Y_t &= \sum_{j=1}^m c_j X_{t-j} + \sum_{j=1}^m d_j Y_{t-j} + \eta_t, \end{aligned} \right\} \quad (3)$$

where  $v_t, \eta_t$  are taken to be two uncorrelated white-noise series. In Eq. (3)  $m$  can equal infinity but in practice, of course, due to the finite length of available data,  $m$  is assumed finite and shorter than the given time series. The definition of causality given above implies that  $Y_t$  is causing  $X_t$  provided some  $b_j$  is not zero. Similarly  $X_t$  is causing  $Y_t$  if some  $c_j$  is not zero. If both of these events occur, there is said to be a feedback relationship between  $X_t$  and  $Y_t$ .

### 3.4 (d) Non-decimated wavelet transform

Wavelets are fundamental building block functions, analogous to the trigonometric sine and cosine functions. Fourier transform extracts details from the signal frequency, but all information about the location of a particular frequency within the signal is lost. In comparison, the multi-resolution analysis makes wavelets particularly appealing for this study, because they are localized in time and the signals are examined using widely varying levels of focus. In this article, we work with non-decimated (discrete) wavelet transform rather than continuous wavelet transform, because from a statistical point of view, they are well adapted (i.e. search for correlations or noise reduction) and offer a very flexible tool for analysis of discrete time series such as the ones under study here. A detailed description of key moments is given in refs. [1,3,4]. The advantages of non-decimated wavelet transform also include (1) a much better temporal resolution at coarser scales than with ordinary discrete wavelet transform, and (2) it allows us to isolate time series of the major components of meteorological signals in a direct way.

## 4. Cross-redundancy and Granger causality for wavelet detail components

Since the wavelet decomposition is an analogue of band-pass filtering, one can be assumed that it provides "pure" separate signals of various periodicity. Our preliminary findings (not presented here) display that the cross-redundancy for high frequency detail components are almost not differed from those for the unfiltered time series. Starting with the 5-year periodicity variations, the cross-redundancies enlarge significantly (in the 3-4 times). Therefore, in this section we consider two low frequency detail components:  $D_5$  with periodicity from 5 to 7 years and  $D_4$  with more than decadal variability.

Figure 1 shows the cross-redundancy and Granger causality for the detailed components  $D_5$ . These components are attractive due to that the ENSO and NAO possess almost same periodicities. In this case, the nonlinear relationship between the teleconnection pattern emerges as a more clear one. First, the cross-redundancy for the AOI and SOI is positive almost everywhere. Also, the Granger causality shows that there is the feedback between these indices during the epochs of the W1 and C at

the lags near 18 months. Second, in contrast with the unfiltered time series, the nonlinear dependence between the AOI and AAOI occurs; in the C epoch it emerges as a feedback at the lags more than 20 months. Third, the feedback is registered for the relationship between the SOI and AAOI, in this case the cross-redundancy amounts to the maximum, and the difference between maxima of cross-redundancy in the epoch of the W1 and C is approximately the 12 months.

Also, the climate forcing of teleconnection pattern (or inverse process) is appeared for the detail components. For example, in the C epoch the temperature anomalies are rather the Granger cause of AAOI, whereas during warming epoch the reverse behaviour is observed.

Furthermore, in the warming epochs the feedback between the T and AOI emerges, but it is not such evident in the case of the SOI. Figure 2 displays the cross-redundancy and Granger causality for the detailed components  $D_5$  with periodicity more than 10 years. Here, the largest (in the mean) and positive values of cross-redundancy are registered. From our point of view, the results obtained for the C epoch are highly notable. The asymmetric behaviour for the interactions between the T, on the one hand, and the indices of the Arctic Oscillation and the Southern oscillation, on the other hand, is observed (see Figs. 2(d) and 2(e)). In other words, when the maximal nonlinear interaction between the T and AOI is registered, the minimal relationship between the T and SOI occurs, whereas the detail components of the AOI and SOI are very similar. At that, in both cases the Granger causality emerges both for maxima and for minima. The cross-redundancies for T-AAOI and SOI-AAOI behave almost similarly, and the nonlinear relationship between the AOI and AAOI, as well as between the AOI and SOI (a lesser degree) varies slightly.

## 5. Conclusions

In this study we use non-fully traditional (for the meteorology) methods to examine the nonlinear interaction between some teleconnection patterns during different epochs of the twenty century. The purpose is to reveal the chaotic behaviour in the global climate system. The main advantage of the cross-redundancy and Granger causality, in contrast to other chaotic analysis, is relatively short time series used as input parameters for these approach. Furthermore, to study the influence of low frequency variations, the wavelet decomposition is applied. By assuming that the non-decimated wavelet transform extract the "pure" low frequency variations, the interaction at the intra- and inter-decadal time scales is considered. By using the results obtained in this paper, we can not conclude that the global warming (or cooling) affect the interaction between the teleconneccion patterns. Of course, the period of exhaustive observation is too short. Moreover, such period with regard to the indices of the Antarctic Oscillation starts in the late 1970s. Therefore, we divide the period from 1910 to 2001 to avoid, as far as possible, the superposition of different epochs that can be observed if to use whole period.

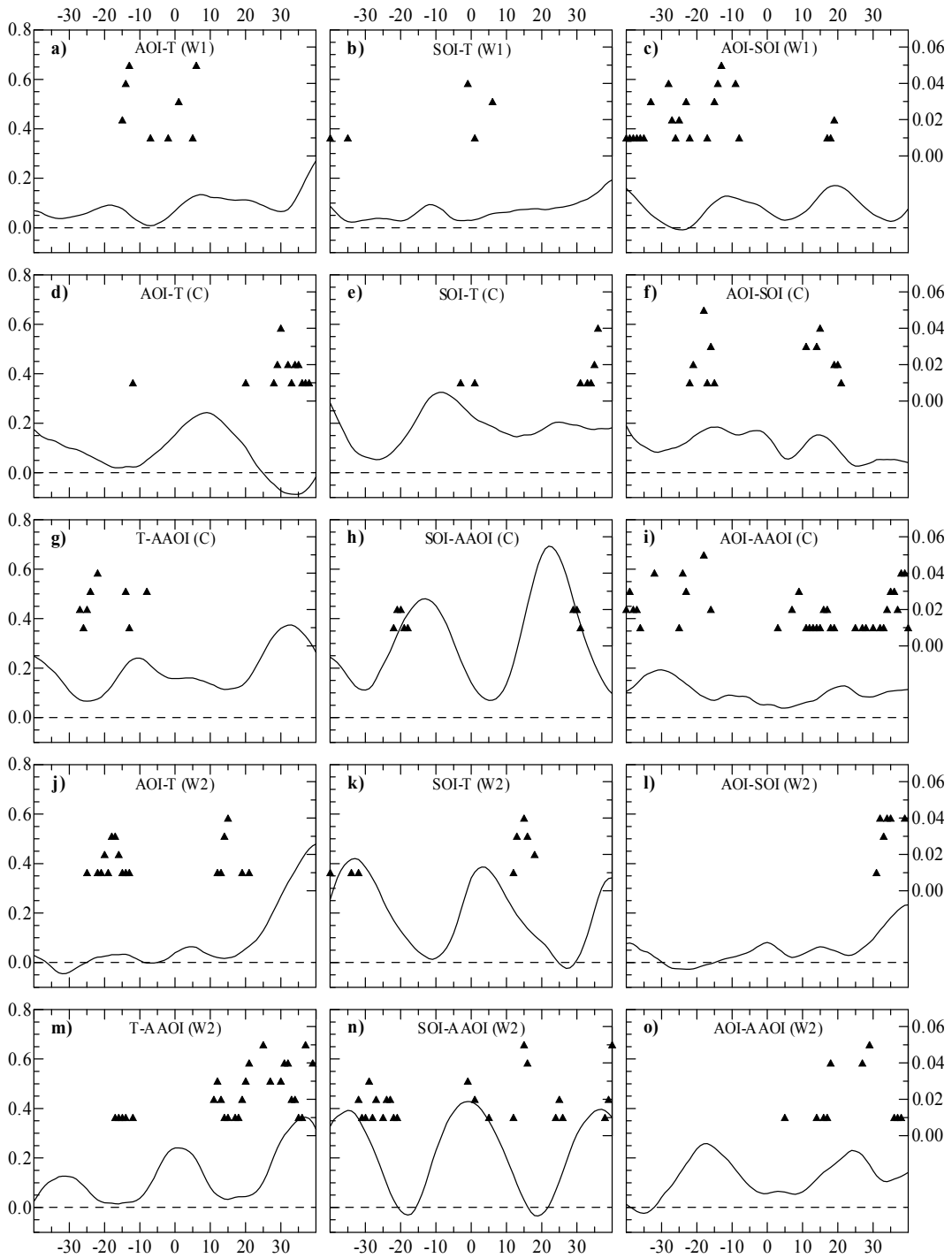


Fig.1. Cross-redundancies (solid lines; left Y-axis) and Granger causalities (triangles; right Y-axis) subject to lag (X-axis) for  $D_5$  for indices of oscillation and global temperature anomalies during 3 epochs

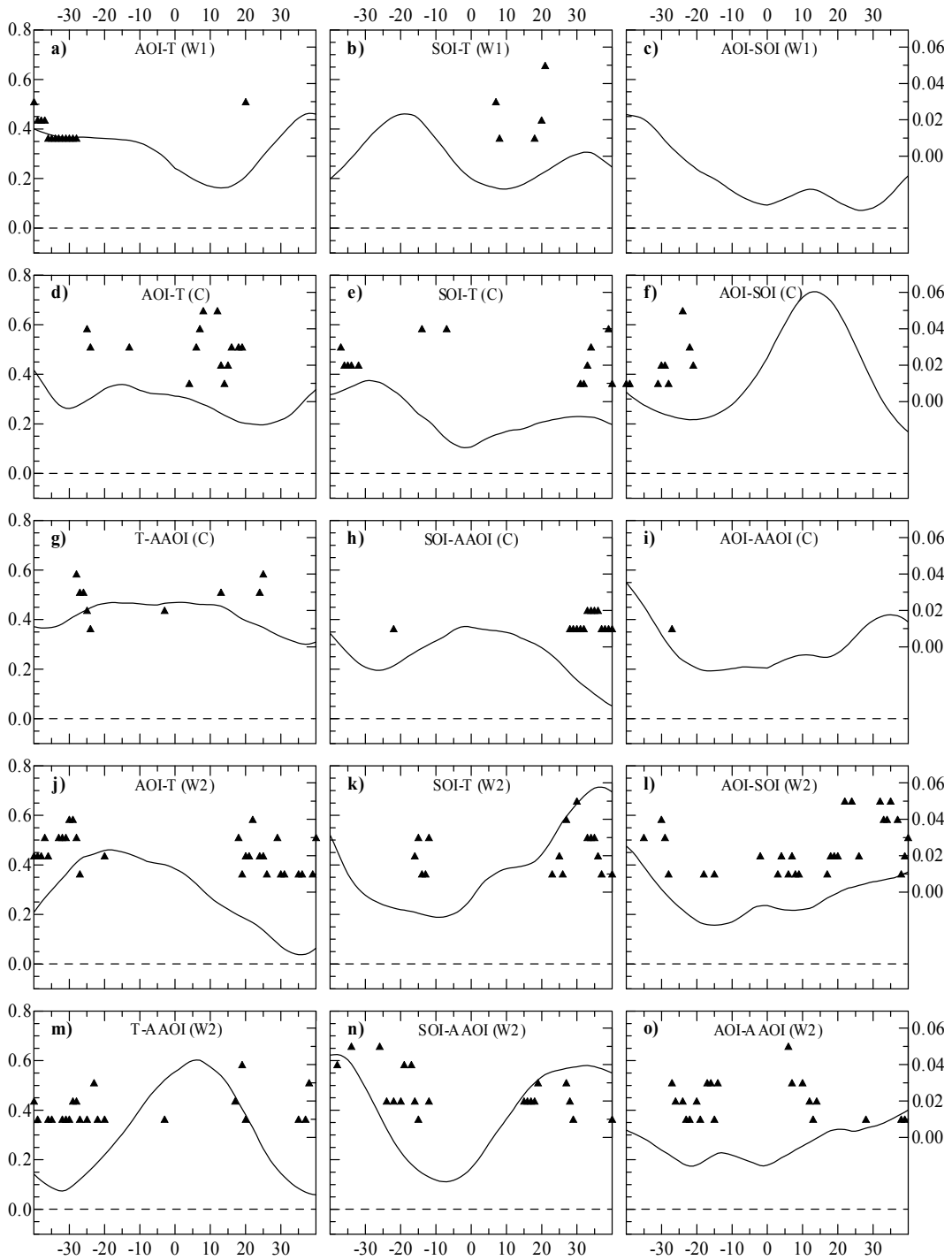


Fig. 2. Cross-redundancies (solid lines; left Y-axis) and Granger causalities (triangles; right Y-axis) subject to lag (X-axis) for  $D_4$  for indices of oscillation and global temperature anomalies during 3 epochs

## References

1. **Glushkov A.V., Khokhlov V.N., Loboda N.S.** Quart. Journ. of Royal Meteorol. Soc., **132**, 447–465 (2006).
2. **Khokhlov V., Glushkov A.V., Tsenenko I.** Nonlin.Proc. in Geophys., **11**, 285–293 (2004).
3. **Loboda N.S., Glushkov A., Khokhlov V., Lovett L.** Journ. of Hydrology, **322**,1–4 (2006).
4. **Glushkov A.V., Khokhlov V.N., Bunyakova Yu.Ya., Prepelitsa G.P., Svinarenko A.A., Tsenenko I.A.** Sensor Electr. and Microsyst. Techn. **3**, N1 21–34 (2006).
5. **Rusov V.D., Glushkov A.V., Khokhlov V.N., Vaschenko V.N., Pavlovich V.N., Tsenenko I.A., Patalaschenko Zh.O.** Вісник Київського ун-ту. Сер фіз.-мат. 4, 471–476 (2004).
6. **Lorenz E. N.** J. Atmos. Sci., **20**, 130 (1963); J. Appl. Meteor., **9**, 325–329 (1970).
7. **Ambaum M.H.P., Hoskins B.J. and Stephenson D.B.** J. Climate, **14**, 3495 (2001).
8. **Ausloos M. and Ivanova K.** Phys. Rev. E, **63**, 047201 (2001).
9. **Cai W. and Whetton P. H.** Geophys. Res. Lett., **27**, 2577–2580 (2000).
10. **da Costa E. D. and de Verdiere A.C.** Q. J. R. Meteorol. Soc., **128**, 797–817 (2002).
11. **Dai A. and Wigley T.M.L.** Geophys. Res. Lett., **27**, 1283–1286 (2000).
12. **Daubechies I.** Ten lectures on wavelets. SIAM, Philadelphia (1992).
13. **Deser K.** Geophys. Res. Lett., **27**, 779–782 (2000).
14. **Diks C. and Mudelsee M.** Phys. Lett. A, **275**, 407–414 (2000).
15. **Duane G. S., Webster P. J. and Weiss J. B.** J. Atmos. Sci., **56**, 4183–4205 (1999)
16. **Eckhardt S., Stohl A., Beirle S. et al.** Atmos. Chem. Phys., **3**, 1769–1778 (2003).
17. **Fyfe J. C., Boer G. J. and Flato G. M.** Geophys. Res. Lett., **26**, 1601–1604 (1999).
18. **Gong D. and Wang S.** Geophys. Res. Lett., **26**, 1601–1604 (1999).
19. **Gouirand I. and Moron V.** Int. J. Climatol., **23**, 1549–1566 (2003).
20. **Granger C.W.** J.Econometrica, **37**, 424–438 (1969)
21. **Grassberger P. and Procaccia I.** Physica D, **9**, 189–208 (1983).
22. **Hannachi A.** J. Climate, **14**, 2138–2149 (2001).
23. **Hu Q., Tawaye Y. and Feng S.** J. Climate, **17**, 1975–1986 (2004)
24. **Hurrell J.W.** Science, **269**, 676–679 (1995).
25. **Kawamura A., McKerchar A. I., Spigel R., Jinno K.** J. Hydrol., **204**, 168 (1998).
26. **Klein S. A., Soden B. J. and Lau N.–C.** J. Climate, **12**, 917–932 (1999).
27. **Li Z.H.** Geophys. Res. Lett., **27**, 3505–3508 (2000);
28. **Lucero O. A. and Rodríguez N.** C Atmos. Res., **54**, 87–104 (2000)
29. **Marshall J., Kushnir Y., Battisti D. et al.** Int. J. Climatol., **21**, 1863–1898 (2001).
30. **Monahan A. H., Fyfe J.C., Flato G.M.** Geophys. Res. Lett., **27**, 1139–1142 (2000)
31. **Nason G., von Sachs R. and Kroisand G.** J. R. Stat. Soc. B, **62**, 271–292 (2000)
32. **Oh H.-S., Ammann C., Naveau P.** J. Atmos. Solar-Terr. Physics, **65**, 191–201 (2003)
33. **Paluš M.** Physica D, **80**, 186–205 (1995); Phys. Lett. A, **213**, 138–147 (1996).
34. **Prichard D. and Theiler J.** Physica D, **84**, 476–493 (1995)
35. **Saito K., Yasunari T. and Cohen J.** Int. J. Climatol., **24**, 33–44 (2004)
36. **Sivakumar B.** Hydrol. Earth System Sci., **4**, 407–417 (2001)
37. **Sutto R.T., Norton W. A. and Jewson S. P.** Atmos. Sci. Lett., **1**, 89–100 (2001)
38. **Thompson D.W. J. and Wallace J.M.** Geophys. Res. Lett., **25**, 1297–1300 (1998)
39. **Torrence C. and Webster P. J.** J. Climate, **12**, 2679–2690 (1999)
40. **Turner J.** Int. J. Climatol., **24**, 1–31 (2004).
41. **Vallis G.K., Gerber E., Kushner P. J., Cash B.J.** Atmos. Sci., **61**, 264–280 (2004).
42. **Voss R. and Mikolajewicz U.** Clim. Dyn., **17**, 45–60 (2001)
43. **Wang C.** ENSO, climate variability, and the Walker and Hadley circulations. The Hadley Circulation: Present, Past, and Future (Eds H. F. Diaz and R. S. Bradley). Springer (2004).